Synthesis and Mesomorphic Properties of Side-Chain Cholesteric Liquid-Crystalline Polysiloxanes

Ying-Ying Zheng, Qian-Yue Li, Bao-Yan Zhang, Li-Feng Zhang

Center for Molecular Science and Engineering, Northeastern University, Shenyang 110004, People's Republic of China

Received 2 August 2004; accepted 3 December 2004
DOI 10.1002/app.21869
Published online in Wiley InterScience (www.interscience.wiley.com).

ABSTRACT: A series of new side-chain cholesteric liquid-crystalline polysiloxanes was synthesized by grafting copolymerization. The chemical structures of the obtained monomers and polymers were confirmed by Fourier transform infrared or ^{1}H-NMR spectroscopy. The mesomorphic properties were investigated with differential scanning calorimetry, polarizing optical microscopy, and X-ray diffraction measurements. The influence of the content of cholesteryl 4-allyloxybenzoate on the phase behavior of the polymers was examined. The monomer 4-(undec-10-en-1-yloxy)-4′-(4-ethoxybenzoyloxy)biphenyl showed nematic and smectic (A, C, and B) phases upon cooling, and cholesteryl 4-allyloxybenzoate revealed an enantiotropic cholesteric phase. One polymer showed a nematic schlieren texture, other polymers showed cholesteric Grandjean and oily-streak textures, and another polymer showed a smectic fan-shaped texture. The experimental results demonstrated that the glass-transition temperature and clearing temperature decreased first and then increased with an increasing content of cholesteryl 4-allyloxybenzoate. © 2005 Wiley Periodicals, Inc. J Appl Polym Sci 97: 2392–2398, 2005

Key words: liquid-crystalline polymer; polysiloxane; synthesis

INTRODUCTION

Research into liquid-crystalline polymers (LCPs) has expanded rapidly in recent years, and polymers with cholesteric structures have attracted considerable interest because they have outstanding optical properties. The helical structure of the cholesteric phase is responsible for this effect: it selectively reflects visible light and exhibits brilliant colors if the pitch of the cholesteric helix coincides with the wavelength of visible light within the material. Because of the angular dependence of the reflection conditions, different observation angles lead to different colors being seen. Furthermore, the reflected light is circularly polarized light, depending on the handedness of the cholesteric helix in the polymer. Just because of the peculiar optical properties, the cholesteric LCPs have many potential applications, such as nonlinear optical filters, flat-panel displays, optical data storage materials, circular polarizers, organic pigments, electrooptic materials, and fast switching materials.[1–12] Cholesteric side-chain LCPs can be obtained by the combination of a mesogenic unit and a chiral component or by the polymerization of chiral mesogenic units.[13–15] The structure of the mesogenic unit, the properties of the chiral unit, and the flexibility and nature of the polymer backbone will influence the liquid-crystalline (LC) properties and orientation states of side-chain chiral LCPs.

Siloxane polymers are materials of significant technological interest. The siloxane bond offers a highly flexible structure, yielding polymer chains with low glass temperatures, low surface tensions, and unique physical and chemical properties.[16–21] Therefore, it would be both necessary and useful to synthesize various kinds of LC polysiloxanes to explore their potential applications.

This article deals with a new preparation method for side-chain cholesteric LCPs. The phase behavior and mesomorphic properties of the monomers and polymers were characterized with differential scanning calorimetry (DSC), polarizing optical microscopy (POM), and X-ray diffraction (XRD) measurements. The influence of the concentration of cholesteryl 4-allyloxybenzoate ($\mathbf{M_2}$) on the phase behavior of the polymers is discussed.

EXPERIMENTAL

Materials

Polymethylhydrosiloxane (PMHS; number-average molecular weight = 700–800) was purchased from Jilin

Correspondence to: B.-Y. Zhang (baoyanzhang@hotmail.com).

Contract grant sponsor: National Natural Science Fundamental Committee of China
Contract grant sponsor: Hi-Tech Research and Development Program (863) of China
Contract grant sponsor: National Basic Research Priorities Programme (973) of China
Contract grant sponsor: Science and Technology Research Major Project of the Ministry of Education of China.

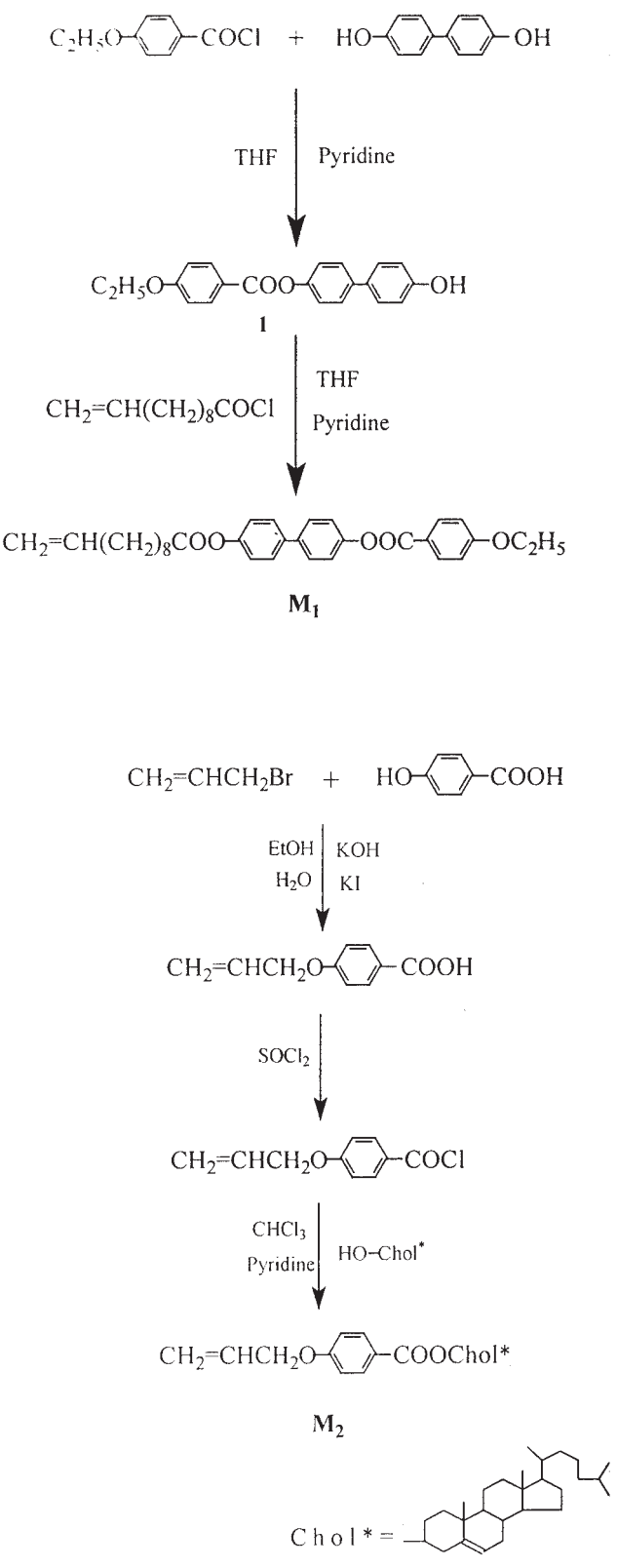

Scheme 1 Synthetic route of the monomers.

Chemical Industry Co. (Jilin, China). Cholesterol was purchased from Henan Xiayi Medical Co. (Zhoukou, China). Undecylenic acid was purchased from Beijing Jinlong Chemical Reagent Co., Ltd. (Beijing, China). 4,4′-Dihydroxybiphenyl (Aldrich, Milwaukee, WI) was used as received. Toluene used in the hydrosilylation reaction was first refluxed over sodium and then distilled under nitrogen. All other solvents and reagents were purified by standard methods.

Measurements

Fourier transform infrared (FTIR) spectra were measured on a Nicolet 510 FTIR spectrometer (Nicolet Instruments, Madison, WI). ^{1}H-NMR spectra (300 MHz) were recorded on a Varian WH-90PFT spectrometer (Varian Associates, Palo Alto, CA). Phase-transition temperatures and thermodynamic parameters were determined with a Netzsch DSC 204 (Netzsch, Hanau, Germany) equipped with a liquid-nitrogen-cooling system. The heating and cooling rates were 10°C/min. The phase-transition temperatures were collected during the second heating. A Leica DMRX (Leica, Wetzlar, Germany) polarizing optical microscope equipped with a Linkam THMSE-600 (Linkam, Surrey, UK) cooling and heating stage was used to observe the phase-transition temperatures and optical textures of the LC monomers and polymers. XRD measurements were performed with nickel-filtered Cu Kα (wavelength = 0.1542 nm) radiation with a DMAX-3A (Rigaku, Tokyo, Japan) powder diffractometer.

Monomer synthesis

The synthesis of the olefinic monomers is shown in Scheme 1.

4-(4-Ethoxybenzoyloxy)-4′-hydroxybiphenyl (1)

4-Ethoxybenzoic acid (8.3 g, 0.05 mol) was reacted at 60°C with 25 mL of thionyl chloride containing a few drops of *N,N*-dimethylformamide for 6 h, and then the excess thionyl chloride was removed under reduced pressure to give the corresponding acid chloride. The acid chloride was dissolved in 10 mL of tetrahydrofuran

TABLE 1
Polymerization

Polymer	Feed (mmol) M_1	Feed (mmol) M_2	M_2 (mol%)[a]	Yield (%)
P_1	7.00	0.00	0.0	87
P_2	6.00	1.00	14.3	85
P_3	5.00	2.00	28.6	76
P_4	4.00	3.00	43.0	79
P_5	3.00	4.00	57.0	74
P_6	2.00	5.00	71.4	76
P_7	1.00	6.00	85.7	78
P_8	0.00	7.00	100.0	74

[a] Molar fraction of M_2 based on M_1 + M_2.

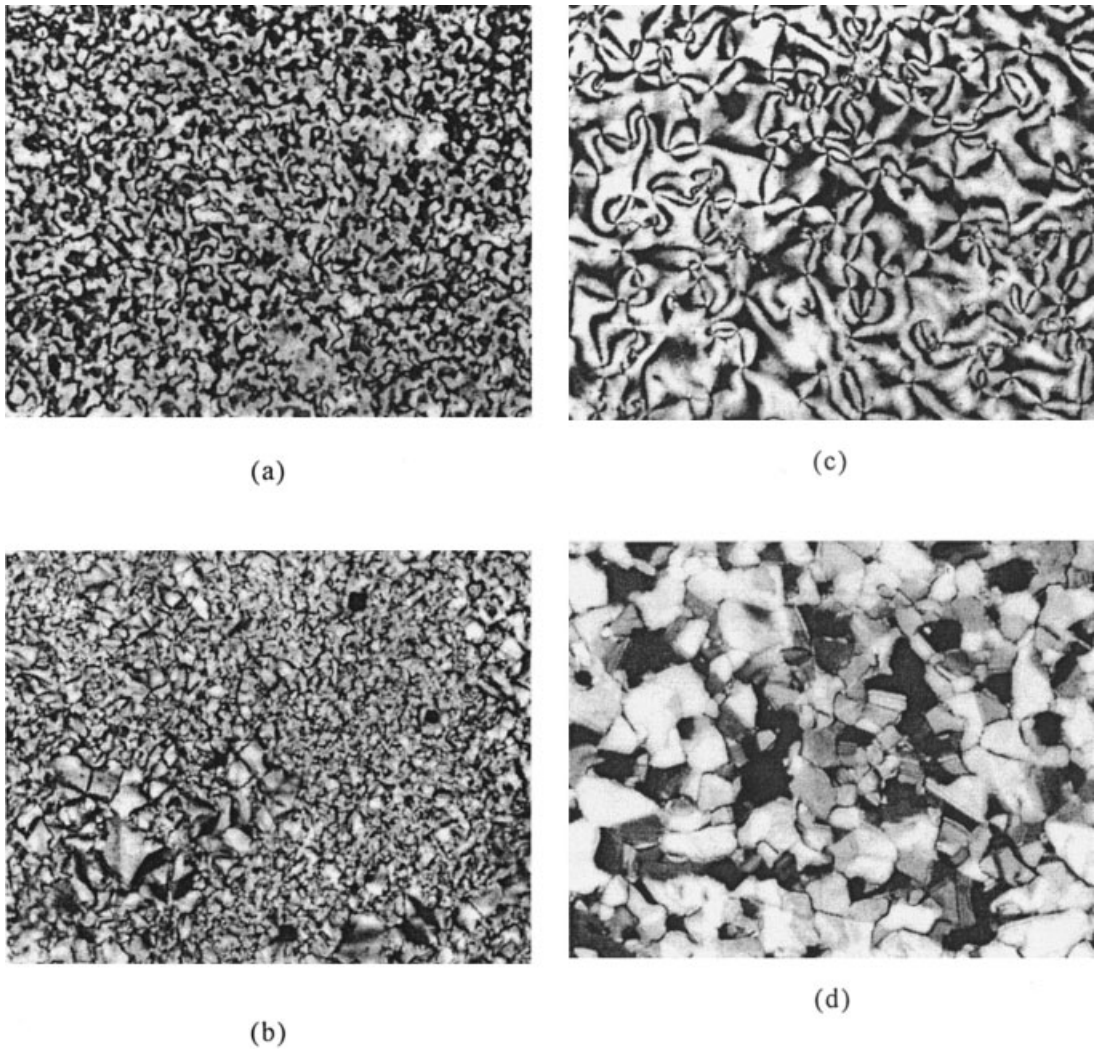

Figure 1 Optical textures of $\mathbf{M_1}$ (200×): (a) threaded texture on heating to 214.6°C, (b) focal-conic texture on cooling to 93.5°C, (c) schlieren texture on cooling to 85.8°C, and (d) mosaic texture on cooling to 83.6°C.

(THF) and then added dropwise to a solution of 55.8 g (0.3 mol) of 4,4′-dihydroxybiphenyl in 200 mL of THF and 20 mL of pyridine under quick stirring. The reaction mixture was refluxed for 15 h. After the removal of the excess solvent, the rest was poured into much water and neutralized with dilute hydrochloric acid. The crude product was obtained by filtration and washed with a 5% sodium hydroxide solution, dilute hydrochloric acid, and cold ethanol successively. The white solid **1** was obtained by recrystallization with acetone.

Yield: 62%. mp: 220°C. IR (KBr): 3443 (—OH), 2983, 2850 (—CH_3, —CH_2—), 1701 (C═O), 1609, 1497 (Ar—), 1264 cm^{-1} (C—O—C). ^{1}H-NMR ($CDCl_3$, tetramethyl silicane (TMS), δ, ppm): 1.33 (m, 1H, —C*H*$_3$), 3.98 (m, 2H, —OC*H*$_2$CH$_3$), 6.79–8.03 (m, 12H, Ar—*H*).

4-(Undec-10-en-1-yloxy)-4′-(4-ethoxybenzoyloxy) biphenyl (m_1)

Undecenyl acid chloride (12.2 g, 0.06 mol) was added dropwise to a solution of 17.2 g (0.05 mol) of compound **1** in 80 mL of THF and 12 mL of pyridine. The reaction mixture was refluxed for 10 h. The precipitate was removed by filtration. Then, the filtrate was poured into cold water and neutralized with dilute hydrochloric acid. After 3 h, the obtained crude product was purified by recrystallization from ethanol. White crystals were obtained.

Yield: 68%. mp: 97°C. IR (KBr): 3075 (═C—H), 2977, 2852 (—CH_3, —CH_2—), 1751, 1731 (C═O), 1641 (C═C), 1604, 1492 (Ar—), 1261 cm^{-1} (C—O—C). ^{1}H-NMR ($CDCl_3$, TMS, δ, ppm): 1.34–1.79 [m, 13H, —C*H*$_3$ and —(C*H*$_2$)$_6$—], 2.03 (m, 2H, ═CHC*H*$_2$—), 2.59 [m, 2H, —(CH$_2$)$_6$C*H*$_2$COO—], 4.12 (m, 2H, —OC*H*$_2$CH$_3$), 4.93–5.08 (m, 2H, C*H*$_2$═CH—), 5.76–5.89 (m, 1H, CH$_2$═C*H*—), 6.97–8.21 (m, 12H, Ar—*H*).

Cholesteryl 4-allyloxybenzoate (M_2)

$\mathbf{M_2}$ was prepared according to similar procedures previously reported.[22]

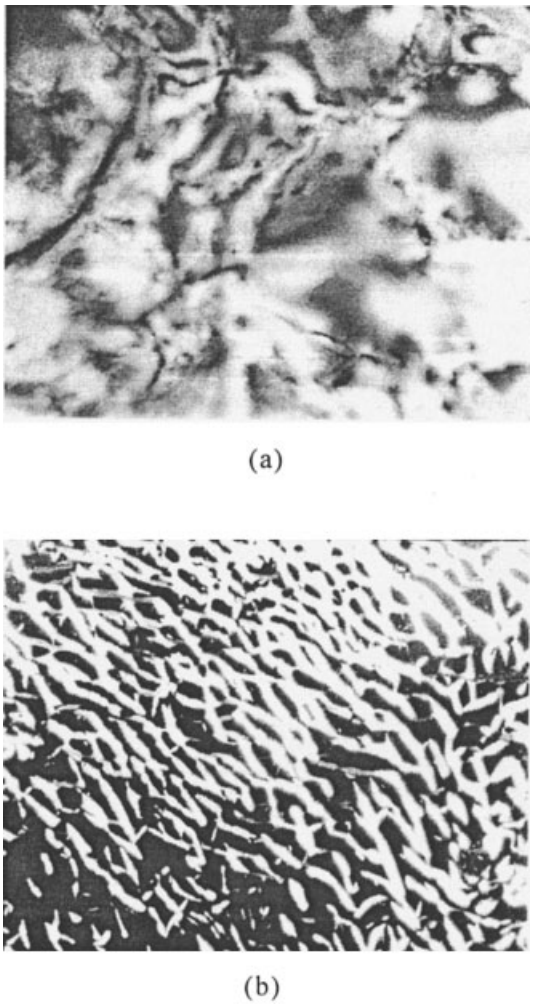

Figure 2 Optical textures of the polymers (200×): (a) schlieren texture of $\mathbf{P_1}$ at 213.5°C and (b) oily-streak texture of $\mathbf{P_4}$ at 270.5°C.

Yield: 72.3%. mp: 107°C. IR (KBr): 3051 (═C—H), 2965, 2854 (—CH_3, —CH_2—), 1735 (C═O), 1634 (C═C), 1606, 1508 cm^{-1} (Ar—). ^{1}H-NMR ($CDCl_3$, TMS, δ, ppm): 0.67–2.03 (m, 43H, cholesteryl-*H*), 4.47 (t, 2H, —OCH_2—), 4.69–5.18 (m, 2H, CH_2═CH—), 5.36 (m, 1H, ═C*H*— in cholesteryl), 6.02 (m, 1H, CH_2═C*H*—), 6.92–7.98 (m, 4H, Ar—*H*).

Polymer synthesis

The polymers $\mathbf{P_1}$–$\mathbf{P_8}$ were synthesized by equivalent methods. For the synthesis of $\mathbf{P_3}$, the monomers $\mathbf{M_1}$ and $\mathbf{M_2}$ and PMHS (feed ratios in Table I) were dissolved in freshly distilled toluene. The mixture was heated to 65°C under nitrogen and anhydrous conditions, and then 2 mL of a THF solution of the hexachloroplatinate(IV) catalyst (5 mg/mL) was injected with a syringe. The hydrosilylation reaction, monitored from the Si—H stretch intensity, went to completion within 48 h, as indicated by IR. After the solvent was removed, the crude polymer was purified by precipitation in toluene with excess methanol and then dried *in vacuo*.

IR (KBr): 2950–2850(—CH_3, —CH_2—), 1757, 1732, 1709(C═O), 1610, 1490 (Ar—), 1150–1000 cm^{-1} (Si—O—Si).

RESULTS AND DISCUSSION

Syntheses

The synthetic routes for the target monomers are shown in Scheme 1. The structural characterization of the monomers and polymers obtained was in good agreement with the prediction. $\mathbf{M_2}$ was prepared according to procedures previously reported by Hu et al.[22] 4-Ethoxybenzoic chloride was reacted with 4,4′-dihydroxybiphenyl in THF in the presence of pyridine, and then $\mathbf{M_1}$ was obtained through the reaction of undecenyl acid chloride with **1** in THF in the presence of pyridine. The FTIR spectra of monomer $\mathbf{M_1}$ showed characteristic bands at 1751–1731 cm^{-1} due to ester C═O stretching, around 1645–1641 cm^{-1} due to vinyl C═C stretching, and around 1604–1492 cm^{-1} corresponding to aromatic C═C stretching. The ^{1}H-NMR spectra of $\mathbf{M_1}$ showed multiplets at 1.28–4.12, 4.93–5.89, and 6.97–8.21 ppm corresponding to methyl and methylene protons, olefinic protons, and aromatic protons, respectively.

The polysiloxanes were prepared by a hydrosilylation reaction between Si—H groups of PMHS and olefinic C═C of $\mathbf{M_1}$ and $\mathbf{M_2}$ in toluene, with hexachlo-

TABLE II
Phase-Transition Temperatures of the Monomers

Monomer	Transition temperature[a] (°C; corresponding enthalpy changes in J/g) Heating / Cooling
$\mathbf{M_1}$	K97.4(66.0)N218.6(3.5)I / 1216.0(3.3)N96.0(2.8)S_A87.9(4.9)S_C84.2(0.5)S_B71.6(24.2)K
$\mathbf{M_2}$	K108.2(42.5)Ch223.7(1.6)I / 1215.7(1.1)Ch74.5(31.3)K

K = solid; N = nematic; S = smectic; Ch = cholesteric; I = isotropic.
[a] Peak temperatures were taken as the phase-transition temperature.

TABLE III
Thermal Properties of the Polymers

Polymer	T_g (°C)	T_m (°C)	ΔH_m (J/g)	T_i (°C)	ΔH_i (J/g)	ΔT[a]	LC phase
$\mathbf{P_1}$	103.4	127.8	5.6	300.2	4.6	172.4	N
$\mathbf{P_2}$	46.5	94.8	4.1	294.2	5.5	199.4	Ch
$\mathbf{P_3}$	40.8	82.1	1.5	285.3	3.8	203.2	Ch
$\mathbf{P_4}$	39.2	76.0	0.6	276.7	2.2	200.7	Ch
$\mathbf{P_5}$	44.2	—	—	266.4	2.0	222.2	Ch
$\mathbf{P_6}$	53.4	—	—	243.5	1.0	190.1	Ch
$\mathbf{P_7}$	62.3	—	—	248.6	0.5	186.3	Ch
$\mathbf{P_8}$	71.6	—	—	278.3	2.7	206.7	S

T_m = melting temperatures, ΔH_m = enthalpy change from solid to LC phase transition, ΔH_i = enthalpy change from LC to isotropic phase transition.
N = nematic; S = smectic; Ch = cholesteric.
[a] Mesophase temperature ranges.

roplatinate(IV) as the catalyst, at 65°C. The IR spectra of the polymers showed the complete disappearance of the Si—H stretching band at 2166 cm^{-1}. Characteristic Si—O—Si stretching bands appeared at 1200–1000 cm^{-1}. In addition, the absorption bands of the ester C═O and aromatic still existed. The polymerization, yields, and solubility of the polymers are summarized in Table I. All the polymers were soluble in hydrocarbons (e.g., toluene and xylene) but were insoluble in hydroxy-group-containing solvents such as methanol and ethanol.

Texture analysis

The optical textures of the monomers and polymers were observed by POM with a cooling and heating stage. POM observations showed that monomer $\mathbf{M_1}$ had an enantiotropic nematic phase and a monotropic smectic phase [smectic A (S_A), smectic C (S_C), and smectic B (S_B)] during its heating and cooling cycles; this agreed with DSC thermograms. When $\mathbf{M_1}$ was heated to about 97.4°C, the typical nematic threaded texture appeared, and the birefringence totally disappeared at 218.6°C. When the isotropic state was cooling to 216.0°C, the threaded texture appeared again. When cooling continued to 96.0°C, the threaded texture changed gradually to the S_A focal-conic texture; when cooling continued to 87.9°C, the S_C schlieren texture appeared; When cooling continued to 84.2°C, the S_B mosaic texture appeared and crystallized at 71.6°C. Monomer $\mathbf{M_2}$ exhibited a cholesteric oily-streak texture and a focal-conic texture during heating and cooling cycles. Photomicrographs of $\mathbf{M_1}$ are shown in Figure 1(a–d).

The cholesteric phase is formed by rodlike, chiral molecules responsible for the macroscopic alignment of cholesteric domains. Polymer $\mathbf{P_1}$ exhibited a nematic schlieren texture. Polymers $\mathbf{P_2}$–$\mathbf{P_7}$ exhibited cholesteric Grandjean and oily-streak textures during heating and cooling cycles. Polymer $\mathbf{P_8}$ exhibited a smectic fan-shaped texture, and the expected cholesteric phase did not appear because the polymer chains hindered the formation of the helical supermolecular structure of the mesogens. Photomicrographs of $\mathbf{P_1}$ and $\mathbf{P_4}$ are shown as examples in Figure 2(a,b).

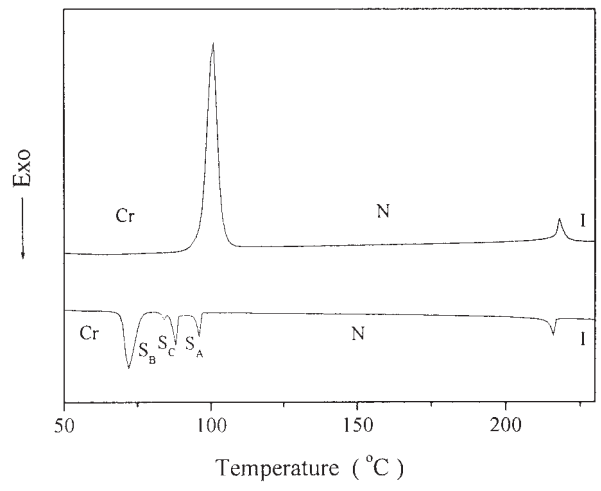

Figure 3 DSC thermograms of monomer $\mathbf{M_1}$.

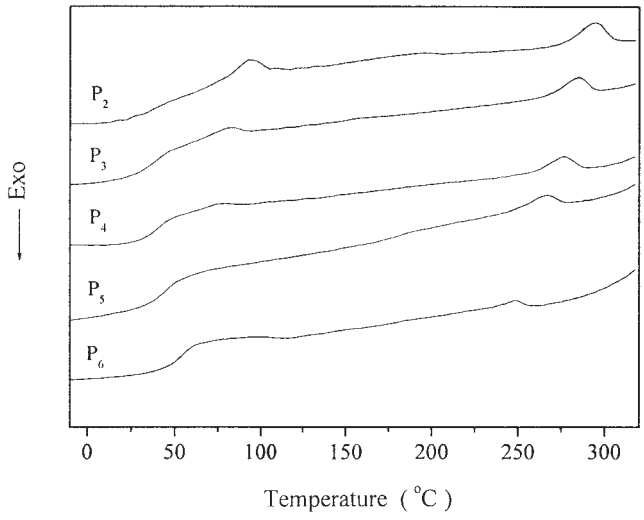

Figure 4 DSC thermograms of the polymers.

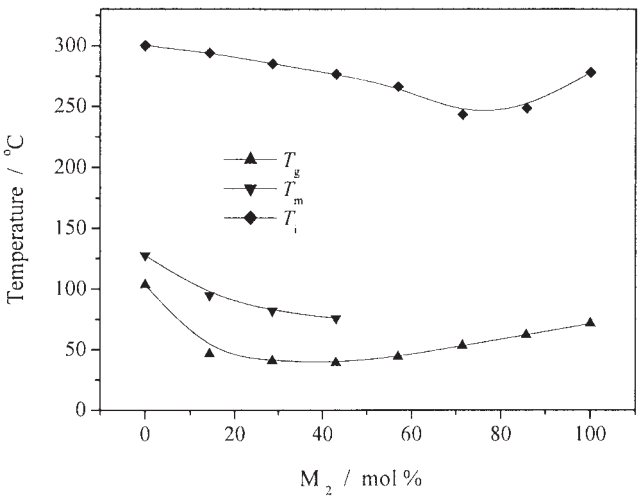

Figure 5 Effect of the $\mathbf{M_2}$ content on the phase-transition temperatures of the polymers.

Thermal analysis

The thermal properties of the synthesized monomers and polymers $\mathbf{P_1}$–$\mathbf{P_8}$ were determined with DSC. The corresponding phase-transition temperatures, obtained during the second heating cycles, are summarized in Tables II and III. Representative DSC curves of the monomers and polymers are presented in Figures 3 and 4.

DSC heating curves of $\mathbf{M_1}$ showed two endotherm peaks, which represented a melting transition and a nematic–isotropic phase transition, respectively. However, during the cooling scan of $\mathbf{M_1}$, five exotherm peaks revealed an isotropic–nematic phase, a nematic–S_A phase, an S_A–S_C phase, an S_C–S_B phase, and a crystallization transition at 216.0, 96.0, 87.9, 84.2, and 71.6°C, respectively. The DSC heating thermograms of $\mathbf{M_2}$ showed a melting transition at 108.2°C and a cholesteric–isotropic phase transition at 223.7°C, respectively. For $\mathbf{P_1}$–$\mathbf{P_4}$, a glass transition at a low temperature, a melting transition, and a mesophase–isotropic transition at a high temperature appeared on DSC curves. This indicated that $\mathbf{P_1}$–$\mathbf{P_4}$ were semicrystalline LCPs. For $\mathbf{P_5}$–$\mathbf{P_8}$, a glass transition and a mesophase–isotropic transition appeared on DSC curves. Above all, the phase transitions were reversible and did not change with repeated heating and cooling cycles.

The glass-transition temperature (T_g) is an important parameter in connection with structures and properties. For side-chain LCPs, T_g is influenced by the nature of the polymer backbone, the rigidity of the mesogenic groups, the length of the flexible spacer, and the copolymer composition. The backbones of side-chain LCPs are primarily polyacrylates, polymethacrylates, and polysiloxanes. However, polyacrylates and polymethacrylates, because of their backbones, show higher T_g's. To obtain mesomorphic properties at a moderate temperature, the polysiloxane backbone and flexible spacer are usually adopted. As we know, T_g involves the mobility of chain segments in polymers, increasing with a decrease in the mobility of chain segments. In polymers $\mathbf{P_1}$–$\mathbf{P_8}$, with the addition of $\mathbf{M_2}$, the symmetry and regularity of the polymers was destroyed, and it reduced the structural heterogeneity; this led to T_g decreasing. However, as the concentration of $\mathbf{M_2}$ continued to increase, the cholesteryl bulky side groups and shorter spacer length of the mesogenic units imposed additional constraints on the motion of the chain segments due to the steric hindrance effect and caused an increase in T_g. Therefore, T_g decreased from 103.4°C for $\mathbf{P_1}$ to 39.2°C for $\mathbf{P_4}$ when the content of $\mathbf{M_2}$ increased from 0 to 43 mol % and then increased from 39.2°C for $\mathbf{P_4}$ to 71.6°C for $\mathbf{P_8}$. Figure 5 shows the effect of the content of $\mathbf{M_2}$ on the phase-transition temperatures of the polymers. Similarly to T_g, the clearing temperature (T_i) of $\mathbf{P_1}$–$\mathbf{P_8}$ first decreased and then increased with an increase in the concentration of $\mathbf{M_2}$ units in the copolymers.

XRD analysis

XRD studies are carried out to obtain more detailed information on the mesogenic phase structure. In general, a sharp and strong peak appears at low angles ($1° < 2\theta < 4°$) in small-angle X-ray scattering (SAXS) curves only for smectic structures; a broad peak associated with lateral packing at about $2\theta = 20°$ is observed in wide-angle X-ray diffraction (WAXD) curves for nematic, smectic, and cholesteric phase structures. Moreover, some research has also shown that a weak peak at $2\theta = 7$–$10°$ is usually observed for a cholesteric structure.[23–26] Figure 6 shows representative XRD curves of quenched samples of the polymers. For $\mathbf{P_8}$, a

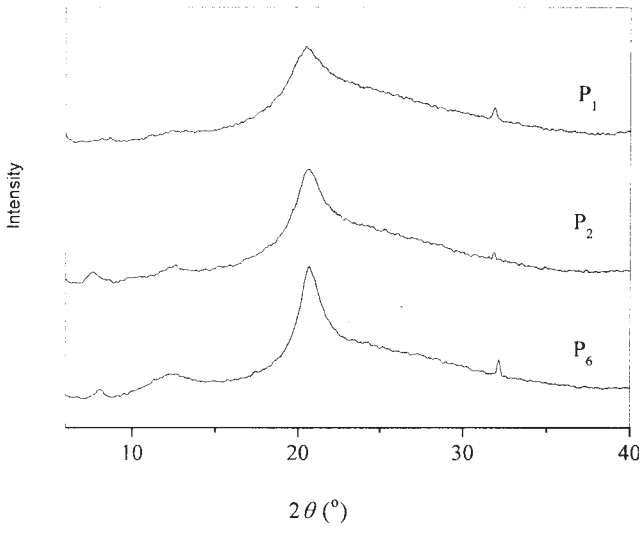

Figure 6 XRD patterns of the quenched samples.

sharp peak associated with the smectic layers in the SAXS curves and a broad peak in the WAXD curves were observed at 2θ values of 1.50 and 22.0°, respectively. According to the Bragg equation, $\lambda_m = 2d \sin \theta$, where λ_m is the wavelength of XRD, the corresponding d-spacings were 6.8 nm^{-1} and 0.4 nm, respectively. For $\mathbf{P_2}$–$\mathbf{P_7}$, no sharp peak at low angles appeared in the SAXS curves, and a weak peak and a broad peak were observed at 2θ values of 8–9 and 21.0–22.0°, respectively, in the WAXD curves. Therefore, the cholesteric structures of $\mathbf{P_2}$–$\mathbf{P_7}$ were confirmed by POM, DSC, and XRD measurements.

CONCLUSIONS

In this study, a series of new side-chain LCPs containing $\mathbf{M_1}$ and $\mathbf{M_2}$ were synthesized and characterized. Monomer $\mathbf{M_1}$ showed nematic and smectic (S_A, S_C, and S_B) phases during cooling, and $\mathbf{M_2}$ revealed an enantiotropic cholesteric phase. Polymer $\mathbf{P_1}$ revealed a nematic phase, $\mathbf{P_2}$–$\mathbf{P_7}$ showed a cholesteric phase, and $\mathbf{P_8}$ revealed a smectic phase. All phase transitions were reversible with repeating heating and cooling cycles. The experimental results demonstrated that T_g and T_i decreased first and then increased with an increasing content of $\mathbf{M_2}$.

References

1. Jacobs, S. D. J Opt Soc Am B 1988, 5, 1962.
2. Belayev, S. V.; Schadt, M. I.; Funfschiling, J.; Malimoneko, N. V.; Schmitt, K. Jpn J Appl Phys 1990, 29, L634.
3. Broer, D. J.; Lub, J.; Mol, G. N. Nature 1995, 378, 467.
4. Bunning, T. J.; Kreuzer, F. H. Trends Polym Sci 1995, 3, 318.
5. Yang, D. K.; West, J. L.; Chien, L. C.; Doane, J. W. J Appl Phys 1994, 76, 1331.
6. Kricheldorf, H. R.; Sun, S. J.; Chen, C. P.; Chang, T. C. J Polym Sci Part A: Polym Chem 1997, 35, 1611.
7. Peter, P. M. Nature 1998, 391, 745.
8. Sapich, B.; Stumpe, J.; Krawinkel, T.; Kricheldorf, H. R. Macromolecules 1998, 31, 1016.
9. Sun, S. J.; Liao, L. C.; Chang, T. C. J Polym Sci Part A: Polym Chem 2000, 38, 1852.
10. Mcdonell, D. G. In Thermotropic Liquid Crystals; Gray, G. W., Ed.; Wiley: New York, 1987; p 120.
11. Bahadur, B. Liquid Crystals: Applications and Uses; World Scientific: Singapore, 1991.
12. Mastrangelo, J. C.; Chen, S. H. Macromolecules 1993, 26, 6132.
13. Takashi, M.; Kazuhiro, N.; Keisuke, F. Polym J 1997, 29, 309.
14. Zhang, B. Y.; Zhi, J. G.; Meng, F. B. Liq Cryst 2003, 30, 1007.
15. Huai, Y.; Hirotsugu, K. Liq Cryst 2002, 29, 1141.
16. Natarajan, L. V.; Bunning, T. J.; Kim, S. Y. Macromolecules 1994, 27, 7248.
17. Hsu, C. S.; Lin, J. H.; Chou, L. R. Macromolecules 1992, 25, 7126.
18. Hsu, C. S.; Shih, L. J.; Hsiue, G. H. Macromolecules 1993, 26, 3161.
19. Hsiue, G. H.; Hsieh, P. J.; Wu, S. L.; Hsu, C. S. Polym Bull 1994, 33, 159.
20. Hsu, C. S.; Chu, P. H.; Chang, H. L.; Hsieh, T. H. J Polym Sci Part A: Polym Chem 1997, 35, 2793.
21. Chiang, Y.; Hong, L. D. J Polym Sci Part A: Polym Chem 2000, 38, 1609.
22. Hu, J. S.; Zhang, B. Y.; Jia, Y. G.; Chen, S. Macromolecules 2003, 36, 9060.
23. Rukmani, S.; Ganga, R. J Polym Sci Part A: Polym Chem 2001, 39, 1743.
24. Dong, Y. M.; Yuan, Q.; Xiao, Z. L. Chem J Chin Univ 1999, 20, 140.
25. Zeng, J.; Huang, Y. Chin J Cellul Sci Technol 2000, 8, 1.
26. Wang, L. G.; Huang, Y. Chin J Cellul Sci Technol 2000, 8, 7.